Poisson's Ratio and Strain Rate Dependency of the Constitutive Behavior of Spinal Dura Mater

CECILIA PERSSON,[1] SAM EVANS,[2] RAINY MARSH,[3] JON L. SUMMERS,[1] and RICHARD M. HALL[1]

[1]School of Mechanical Engineering, University of Leeds, Leeds LS2 9JT, UK; [2]School of Engineering, Cardiff University, Cardiff CF24 3AA, UK; and [3]Faculty of Biological Sciences, University of Leeds, Leeds LS2 9JT, UK

Associate Editor Sean S. Kohles oversaw the review of this article.

Abstract—Knowledge of the mechanical behavior of spinal dura mater is important for a number of applications including the experimental and computational modeling of physiological phenomena and spinal cord trauma. However, mechanical characterization of dura mater is relatively sparse and is further compounded by the use of the tangent modulus as the sole measure of stiffness. This study aims to provide a more complete description of the mechanical properties of spinal dura mater, including the effect of strain rate. Bovine dura mater was tested under uniaxial tension in both the longitudinal and the circumferential directions at three different strain rates; 0.01, 0.1, and 1.0 s^{-1}. An Ogden model was fitted to the resulting stress–stretch data. The morphology of the dura mater was assessed using Sirius red and H&E staining. No significant effect of the strain rate was found for the Ogden model parameters. Longitudinal specimens were significantly stronger and more deformable than circumferential samples, probably due to the structural arrangement of the collagen fibers. At low strains, however, the circumferential specimens were stiffer than the longitudinal ones. The findings of this study will allow more complete representations of the spinal dura mater to be developed.

Keywords—Spinal dura mater, Material properties, Circumferential, Longitudinal, Strain rate, Poisson's ratio.

INTRODUCTION

The spinal dura mater encases the cerebrospinal fluid and protects the sensitive spinal cord. It is composed mainly of collagen and elastin fibers which form an extracellular matrix that has been found to exhibit viscoelastic material behavior under deformation.[10,20] Studies on other viscoelastic soft tissues have found a variation in mechanical behavior with strain rate[5] but to the authors' knowledge, the effect of rate of deformation on the dura mater has not been investigated. Due to the anisotropic structure of the dura mater, in which the collagen fibers have been found to be arranged with a longitudinal tendency,[10,13,15] it is important to evaluate the mechanical behavior in both directions.

Previous studies on the mechanical properties of dura mater have tended to report a single tangent modulus at a lone—sometimes unknown—strain rate,[13,15,16,18,20] whereas in reality the stiffness of the dura varies with the amount of strain and possibly with strain rate. This lack of adequate characterization is further compounded by the scarcity of data relating to the Poisson's ratio. Hence, a more complete characterization of the dura's mechanical properties is required if models are to be successfully deployed in furthering our understanding of the complex interactions among the cord, CSF, and para-spinal tissues. The aim of this study was to evaluate the constitutive behavior of dura mater, including Poisson's ratio and strain-rate dependency, under uniaxial tension in both the longitudinal and the circumferential directions. Histology was used to relate the structure of the tissue to its mechanical performance.

MATERIALS AND METHODS

Sample Preparation

Bovine specimens were obtained from cattle aged 16–24 months. Samples with intact dura were liberated from excess fat and the dura was removed from the cord. A custom-made dumb-bell-shaped cutter and a press were used to produce specimens in both the longitudinal and the circumferential directions,

Address correspondence to Richard M. Hall, School of Mechanical Engineering, University of Leeds, Leeds LS2 9JT, UK. Electronic mail: R.M.Hall@leeds.ac.uk, K.C.Persson@leeds.ac.uk
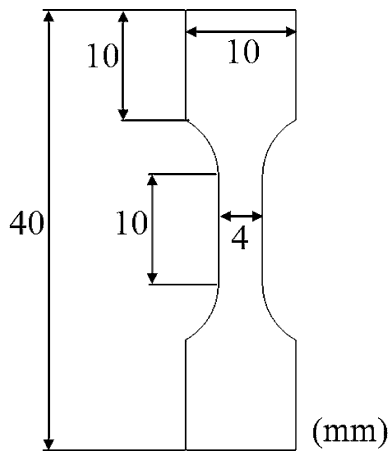
FIGURE 1. Specimen dimensions for uniaxial tensile testing.

TABLE 1. Group designations and number of specimens per strain rate and direction.

Group	Strain rate (s^{-1})	Direction	Number of specimens
0.01C	0.01	Circumferential	7
0.1C	0.1	Circumferential	10
1.0C	1.0	Circumferential	4
0.01L	0.01	Longitudinal	6
0.1L	0.1	Longitudinal	6
1.0L	1.0	Longitudinal	5

ensuring that the central part of the specimen consisted of anterior dura (Fig. 1), which is the region on which a burst fracture fragment impinges.[1] Twenty cords were used to produce four to ten specimens per group (Table 1). The width and the thickness were measured to a precision of 10 μm with a traveling microscope (W.G. Pye & Co Ltd., Cambridge, UK) and a micrometer (No 2050-08, Mitutoyo, Andover, UK), respectively. The specimens were wrapped in paper tissue soaked in saline solution and stored at −20 °C. Before testing they were stabilized at room temperature. This method of storage has been found to have no significant influence on the mechanical properties of bovine dura mater.[15] The specimens were kept moist with saline solution throughout preparation and testing.

Mechanical Testing

Custom-made soft tissue specimen clamps were used together with a back-piece holding a 25-mm separator to ensure axial alignment of the specimen. No pre-strain was used as it can vary considerably (from 0 to 15%) throughout the spinal length and there is no consensus on the value to be used.[14,16] Specimens were preconditioned for 10 cycles at 15 mm/min up to
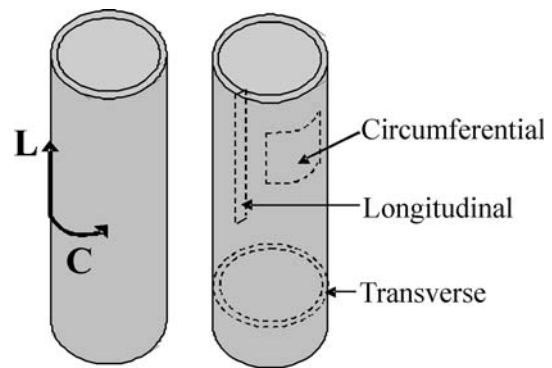

FIGURE 2. Dura mater. (Left) Longitudinal and circumferential specimen directions for mechanical testing. (Right) Where the histology sections were taken and how they were defined.

6(±1.5)% deformation (similar to physiological strains[14,22]) before being stretched to failure. Three nominal displacement rates were used: 15, 150, and 1500 mm/min to give three strain rates: 0.01, 0.1, and 1.0 s^{-1}, corresponding to a large range of strain rates. The materials' testing machine used (Losenhausen Maschinenbau, Dusseldorf, Germany) was equipped with an MTS Flex Test GT controller (MTS, Eden Prairie, MN, USA) and a 100 N load cell. For the two lowest strain rates, the tests were recorded at 5 Hz with a Correlated Solutions digital image correlation system (Limess GmbH, Pforzheim, Germany) which also recorded the load using Limess software. For the highest strain rate, the tests were recorded at 62 Hz with a high-speed video camera (Motioneer, AOS Technologies AG, Baden Daettwil, Switzerland) synchronized with the load cell via a trigger signal from the MTS controller, which recorded the load and displacement. The accuracy of the two methods was verified at the lower strain rates and they were found to produce the same load (±1%) at a given time. The group designations and the number of specimens tested per strain rate and direction are displayed in Table 1. Specimen directions are defined in Fig. 2.

Data Analysis

The deformation of the specimens was calculated from the video images using MATLAB (R2006b, Mathworks Inc., Natick, MA, USA). The average of three pairs of markers per direction was used to evaluate the strain in each specimen. Since significant cross-sectional area variations were expected, the true stress and strain were calculated as

$$\sigma_t = (1 + \varepsilon_e)\sigma_e \tag{1}$$

and

$$\varepsilon_t = \ln(1 + \varepsilon_e) \tag{2}$$

respectively, where

$$\sigma_e = \frac{F}{A_0} \quad (3)$$

and

$$\varepsilon_e = \frac{\Delta l}{l_0} \quad (4)$$

are the engineering stress and strain, respectively.

Typical stress–strain curves for both specimen directions are shown in Fig. 3. The curves can be divided into two approximate phases: A–B, where the majority of recruitment and alignment of crimped collagen fibers occur, and B–C, in which a significant number of fibers have been recruited and are stretched.[15] The point B can be found by fitting a straight line to the most linear portion of the curve prior to failure and taking its intersection with the x-axis. Poisson's ratio was calculated separately for each phase—as an average of all values within that phase—using the following equation for each data point:

$$v = -\frac{\varepsilon_x}{\varepsilon_y} \quad (5)$$

The stress–stretch data was fitted using MATLAB to an Ogden model[10,12] for simple tension of an incompressible material:

$$\sigma = \frac{2G}{\alpha}(\lambda^{\alpha-1} - \lambda^{-0.5\alpha-1}) \quad (6)$$

where σ is the engineering stress, λ the stretch (the ratio of the current length to the original length, l/l_0), and G and α are the material parameters. G corresponds to the instantaneous shear modulus of the tissue and α defines the exponential part of the stress–stretch curve and is also related to the stiffness. The stiffness of the material is defined as the change in stress required for a change in deformation:

$$\frac{\partial\sigma}{\partial\varepsilon} = \frac{\partial\sigma}{\partial\lambda}\frac{\partial\lambda}{\partial\varepsilon} = \frac{\partial\sigma}{\partial\lambda} * 1$$
$$= \frac{2G}{\alpha}\big((\alpha-1)\lambda^{\alpha-2} + (0.5\alpha+1)\lambda^{-0.5\alpha-2}\big) \quad (7)$$

Since the Ogden model is a hyperelastic model with no viscous term, a strain rate dependency would manifest itself as a change to the Ogden parameters.

Statistical Analysis

Statistical analysis of the results was performed using a general linear model with specimen direction and strain rate as fixed factors (equivalent to a two-way ANOVA) in SPSS (SPSS 16.0, SPSS Inc., Chicago, IL, USA). Since a normal distribution and homoscedasticity could not be verified for all variables, the data were ordered by ranks before statistical testing. For Poisson's ratio, phase was added to the fixed factors, giving a three-way analysis. All analyses were made to a significance level of 0.05.

Histology

Sample preparation was completed in the same manner as for the experimental specimens. Samples were fixed overnight in 10% (v/v) Nutrient Buffered Formalin (NBF) prior to automated tissue processing (Leica TP 1020, Leica Microsystems, Milton Keynes, UK) under the following conditions: 10% NBF (1 h), 70% ethanol (1 h), 90% ethanol (1 h), 100% ethanol (3× 1 h), xylene (3× 1 h), molten wax (3× 1 h). Sections of dura were embedded in wax blocks so that longitudinal, circumferential, and transverse sections could be analyzed (Fig. 2). 5 and 10 μm sections were cut using a microtome and dried for 1 h at 37 °C. Sections were dewaxed in xylene (2× 5 min) then rehydrated in 100% ethanol (3× 2 min). Following 1 min in 70% ethanol, slides were washed in water. The cellular and collagen structures of the dura were visualized by staining with Hematoxylin and Eosin (H&E, Bios Europe, Skelmersdale, UK) and 0.1% Sirius red F3B (Raymond A Lamb, Eastbourne, England) in saturated picric acid, using standard protocols. Stained and washed sections were dehydrated in 70% ethanol (10 s) followed by 100% ethanol (3× 1 min). Slides were cleared in xylene (2× 1 min) and cover slips mounted using DPX mounting medium (Bios Europe Ltd., Edinburgh, UK.). Sections were visualized using a light microscope and images captured digitally. Twelve images were analyzed in ImageJ (ImageJ 1.37v, NIH, USA) to evaluate the fiber angles and the crimp of the fibers. One fiber per bundle was
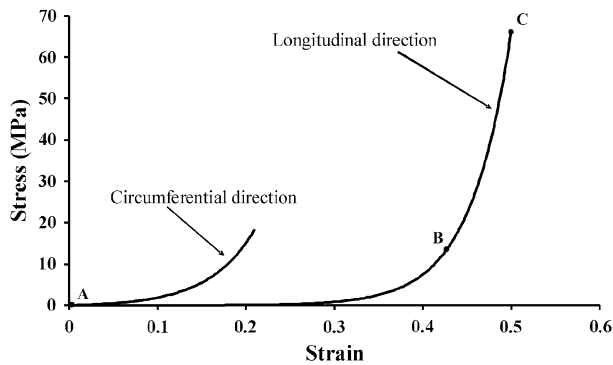
FIGURE 3. Typical stress–strain curves for the circumferential and the longitudinal directions. Point B is defined by the intersection of the x-axis with the tangent to the latter part of the curve.

segmented into straight lines and the crimp was calculated as the ratio of crimped (segmented) length to straight length. A total of 28 fibers were used to calculate the crimp.

RESULTS

Mechanical Testing

The video images confirmed the mean and standard deviation of the nominal strain rates to be $0.011(\pm 8 \times 10^{-4})$, $0.11(\pm 0.01)$, and $1.1(\pm 0.1)$ s^{-1}.

Representative raw stress–stretch curves for the two test directions are shown in Fig. 4. Whereas the longitudinal specimens typically failed at the maximum load in an instantaneous manner, the circumferential specimens typically continued to carry load as not all fibers failed simultaneously. Each group's average constitutive model is plotted in Fig. 5 and the model
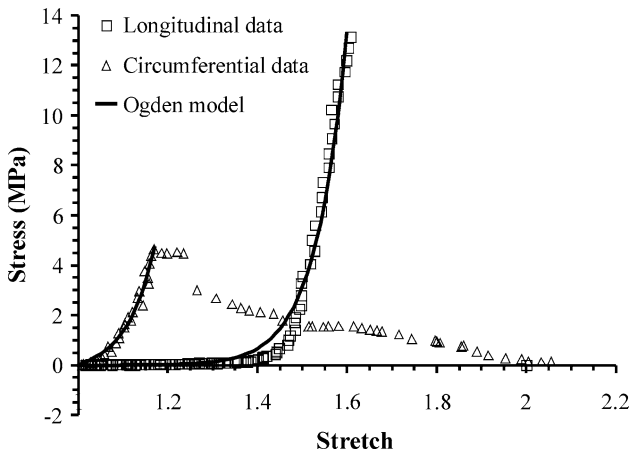
parameters are shown in Figs. 6 and 7. The Poisson's ratio and the maximum true stresses and strains before loss of structural integrity (determined from the video images and a notable force drop) are shown in Figs. 8–10.

The specimen direction (circumferential vs. longitudinal) had a statistically significant effect on all variables as shown in Table 2. However, the strain rate showed a statistically significant influence on the maximum strain and Poisson's ratio only, although no particular trends could be discerned. The *post hoc* tests found a significant difference only between 0.01 and 0.1 s^{-1} for Poisson's ratio (Scheffe's test, $p = 0.045$). Poisson's ratio was found to be significantly higher in phase B–C than phase A–B ($p < 0.001$, Table 2).

Histology

Both the longitudinal and the circumferential sections, which were stained for collagen, showed individual fibers aligned in both of these directions (Figs. 11a–11c). However, circumferentially aligned
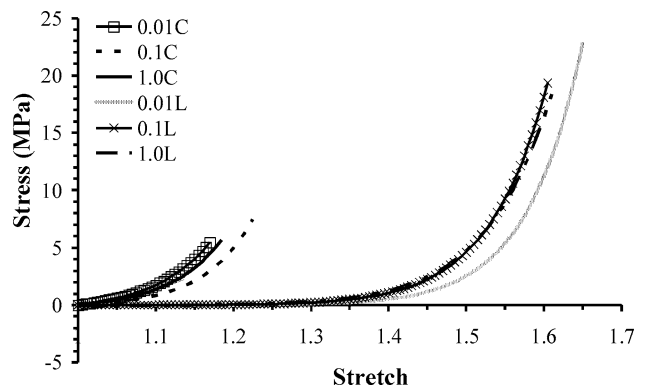

FIGURE 4. Representative raw stress–stretch data and model fits for the two specimen orientations (circumferential and longitudinal).

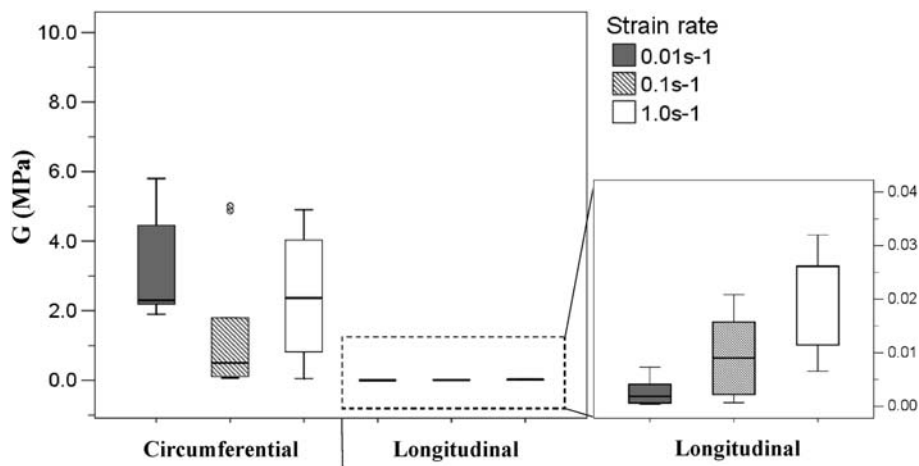**FIGURE 5. Average Ogden models with equations $\sigma = (2G/\alpha)(\lambda^{\alpha-1} - \lambda^{-0.5\alpha-1})$.**

FIGURE 6. Results for Ogden model parameter *G*. Longitudinal results are magnified for clarity. ° denotes outliers.
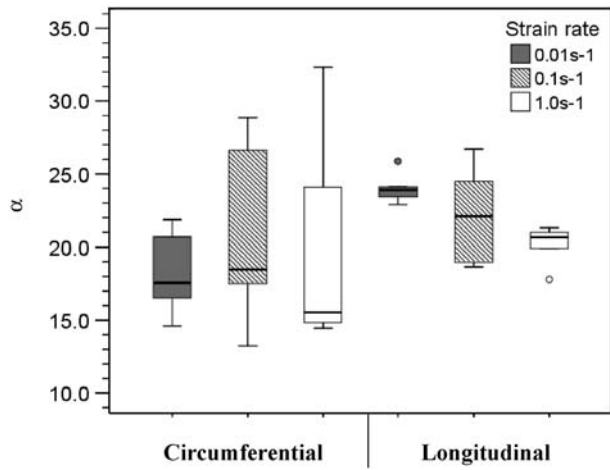
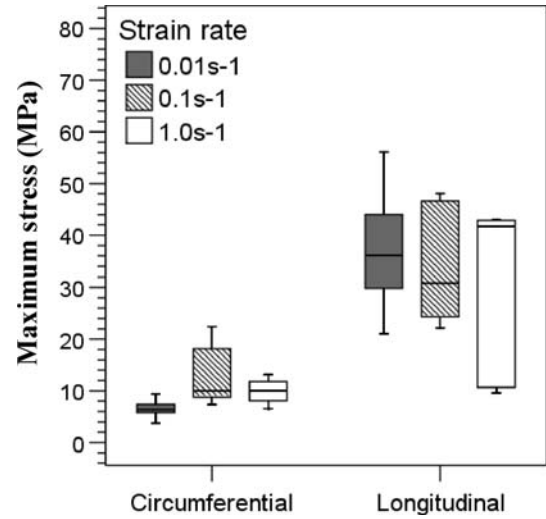FIGURE 7. Results for Ogden model parameter α. ° denotes outliers.

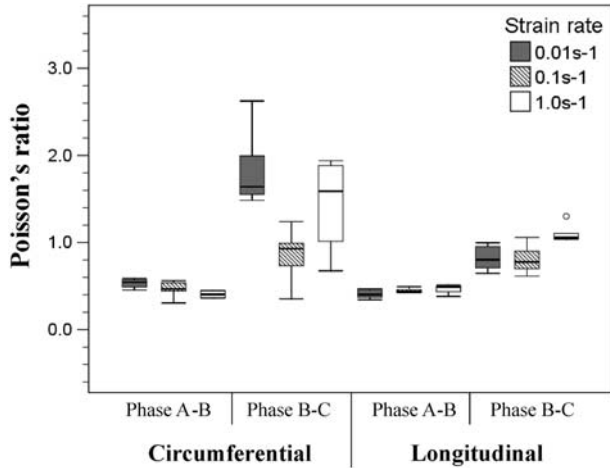FIGURE 9. The true maximum stress before the loss of structural integrity for specimen orientation and strain rate.

FIGURE 8. Poisson's ratios for the two different specimen orientations (circumferential and longitudinal) and for the different phases A–B (disentanglement) and B–C (fiber stretching) (cf. Fig. 3). ° denotes outliers and + extreme cases.
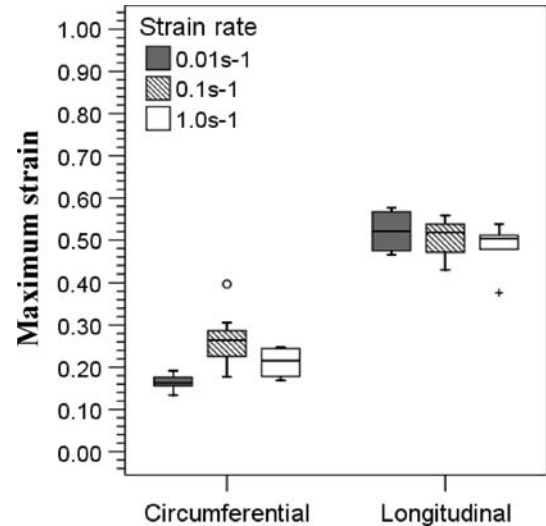

FIGURE 10. The true maximum strain before the loss of structural integrity for specimen orientation and strain rate. ° denotes outliers and + extreme cases.

TABLE 2. p-values for the statistical analysis results.

	G	α	Maximum stress	Maximum strain	Poisson's ratio
Direction (circumferential or longitudinal)	<0.001*	0.01*	<0.001*	<0.001*	0.005*
Strain rate (0.01, 0.1, and 1.0 s^{-1})	0.21	0.30	0.10	0.02*	0.02*
Phase (A–B or B–C)	N/A	N/A	N/A	N/A	<0.001*

*Statistically significant at 0.05.

fibers were less crimped than the longitudinally aligned ones: the crimped-to-straight length ratio was found to be 1.21($\pm$0.07) for the circumferential fibers and 1.66($\pm$0.31) for the longitudinal fibers. Circumferentially aligned fibers seemed to be located mainly at

the outer edge of the dura, whereas the longitudinal ones were located toward the middle and close to the arachnoid edge (Figs. 11a–11c). The transverse sections also showed different fiber directions (Fig. 11d), although fibers appeared to be predominantly arranged
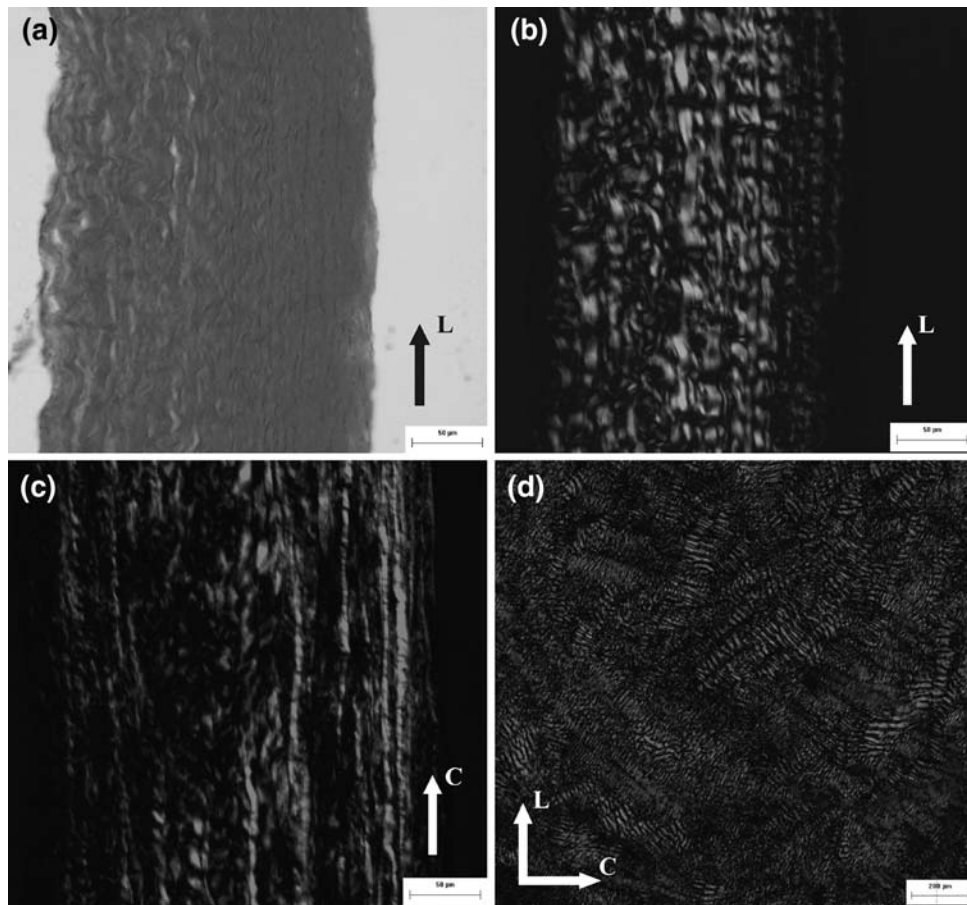
FIGURE 11. Sirius red collagen staining: (a) a longitudinal section; (b) the negative image of the same longitudinal section showing crimped fibers in the longitudinal direction; (c) a transverse section showing fibers in the circumferential direction; (d) a circumferential section showing crimped fibers arranged in different directions. Arrows indicate longitudinal and circumferential directions (as defined in Fig. 2). (a–c) The outer edge of the dura is to the right and the arachnoid edge is to the left.

in a longitudinal manner. These other fiber directions were approximately at a 48° and 142° angle (where the circumferential and the longitudinal directions are defined at 0° and 90°, respectively), and presented a crimp to straight length ratio of 1.21($\pm$0.06) and 1.40($\pm$0.20), respectively.

The H&E staining demonstrated that a proportion of—but not all —cells were aligned with the fiber direction (Fig. 12). The discordance between cell and fiber alignment may be due to the fact that some cells were aligned with fibers that have a predominant direction which is orthogonal to the image. The transverse section also showed cells aligned in similar directions to the fibers in Fig. 11d.

DISCUSSION

This study assessed the mechanical and the structural properties of bovine dura mater by performing uniaxial tensile tests as well as histological staining.

The study was prompted by an unavailability in the literature of a more thorough description of the constitutive behavior of dura mater, in particular at different strain rates.

No statistically significant effect of the strain rate on the Ogden model parameters was found in this study. Although G increased with the strain rate for the longitudinal specimens, indicating an increase in stiffness, a significant difference could not be found. The dura mater has been found to present viscoelastic properties,[10,13,20] and a strain-rate dependency could therefore be expected. However, although previous studies on other viscoelastic tissues such as the human spinal cord[2] and the rat spinal cord[5] also found a trend in increasing stiffness with strain rate, considerable experimental variability and no statistical significance were reported. Yet another study on the human spinal cord found no difference in stiffness due to a 100-fold increase in strain rate.[11] Furthermore, research on other collagen-rich tissues such as the canine[21] and the rabbit[3] medial collateral ligament have found similar
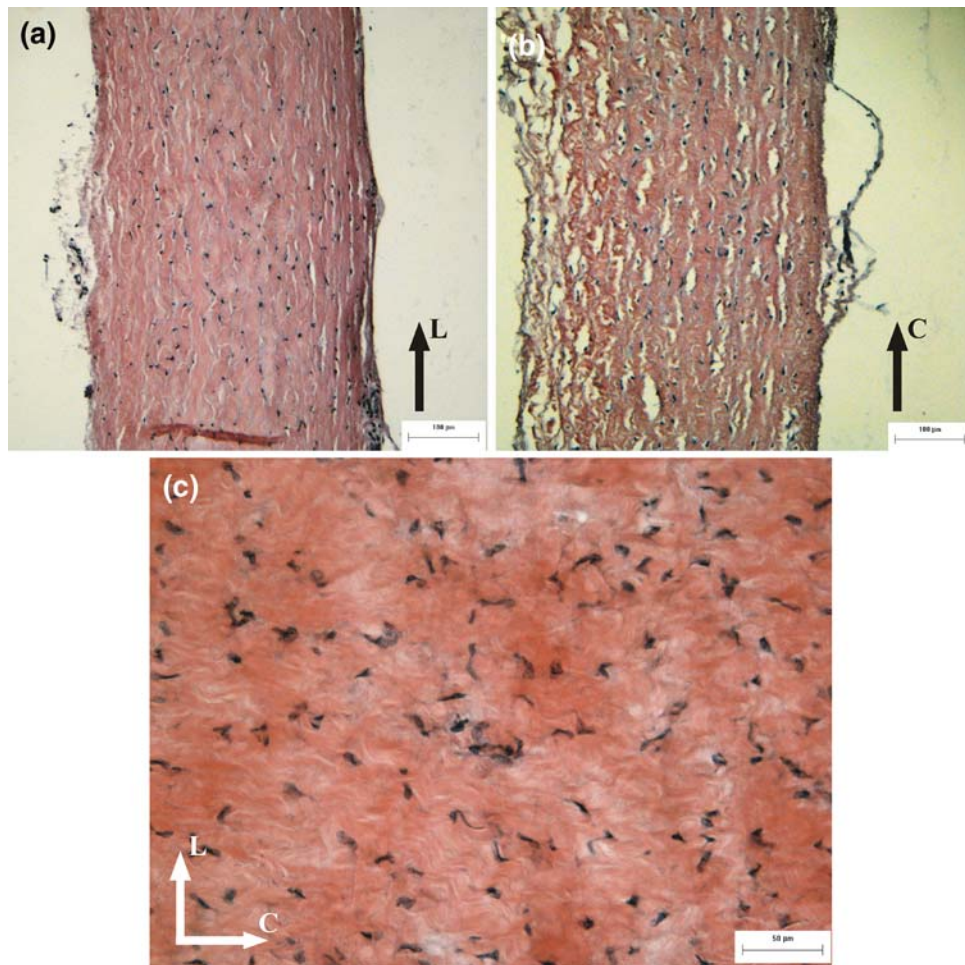
FIGURE 12. H&E stained (a) longitudinal section, (b) transverse section, and (c) circumferential section, all showing aligned as well as non-aligned cells with respect to the fiber orientation. Arrows indicate longitudinal and circumferential directions (as defined in Fig. 2). (a, b) The outer edge of the dura is to the right and the arachnoid edge is to the left.

results. In the study by Woo *et al.*[21] on the canine medial collateral ligament, the experimental values were found to overlap the predicted results at a 100 times higher strain rate. In the study by Crisco *et al.*[3] on the rabbit medial collateral ligament, only an average 24% increase in stiffness was found due to a raise in strain rate from 0.01 to 36.6 s^{-1} and 140 s^{-1} (no difference was found in the results for the two highest strain rates). This indicates that the natural variability in these tissues may mask the effect of a 100-fold increase in strain rate.

Comparing the two specimen directions, it was found that G was significantly higher for the circumferential than the longitudinal direction, and α tended to be slightly lower in the circumferential direction. This implies that for a given amount of strain, the circumferential specimens had a higher stiffness than the longitudinal specimens. However, since the circumferential specimens ruptured at a lower strain, the stiffness at 85% of the maximum strain of a specimen was similar for both directions, and at 90% of maximum strain the stiffness of the longitudinal specimens was significantly higher than that of the circumferential specimens. This is in agreement with Runza *et al.*'s[15] study on human dura specimens, where the stiffness of the last 10% deformation before failure was measured, and the longitudinal specimens were found to be significantly stiffer than the circumferential ones. Wilcox *et al.*[20] evaluated the stress relaxation properties of bovine dura mater under low strains, and found a higher stiffness in the circumferential direction than in the longitudinal direction, also in accordance with this study. The lower stiffness of the longitudinal specimens at lower, *in vivo* strains, could reflect the need for deformability in this direction as the neck is flexed for example, whereas in the circumferential direction the dura only needs to accommodate the pulsatile

flow of the cerebrospinal fluid.[9] The lower values of G of the longitudinal specimens also reflected the longer phase of recruitment of the collagen fibers, again allowing for greater deformability. This might be due to the preferential alignment of the collagen fibers in this direction as well as an increased amount of crimping of these fibers, as indicated by the histology results.

In terms of Poisson's ratio, all three factors (direction, strain rate, and phase) were found to have a significant effect on the results, although no particular trend could be discerned as regards the strain rate. With respect to phase AB, Poisson's ratio was higher for both circumferential and longitudinal specimens in phase BC. To the authors' knowledge, the Poisson's ratio of dura mater has not been reported previously, but it has been shown elsewhere that Poisson's ratios of anisotropic materials can be unbounded.[17] Average values for other anisotropic collagen-rich soft tissues such as the hip joint ligaments[7] and patella cartilage[4] are similar (1.1–2.0 and 0.6–1.9, respectively) to those of the second phase of this study, and present ranges that encompass also the first phase.[7]

With regard to the maximum stress and the maximum strain, again no particular trend was found with respect to the strain rate. The maximum stresses and strains were higher for the longitudinal specimens compared to the circumferential specimens. This higher strength and deformability of the longitudinal specimens are most likely due to the structural arrangement of the collagen fibers, since they are the strongest and most dominant component of the material. Runza *et al.*[15] also found a higher maximum stress for human longitudinal dura samples compared to circumferential ones, but no difference as regards the maximum strain. Runza *et al.* also tested bovine specimens (in the longitudinal direction only), and found similar results to this study.

Whereas the present results were similar to those found in previous studies on bovine dura mater,[15,20] the parameters found for the Ogden model in the circumferential direction were similar to the results from the study by Maikos *et al.*[10] on rat dura mater in the other, longitudinal direction ($G = 1.20 \pm 0.79$ MPa and $\alpha = 16.2 \pm 9.7$). However, there were differences in the shape of the load–deformation curve compared to the results of this study, which may account for the different values of G and α. In particular, the curves presented for the rat dura mater[10] showed post-yield deformation at an increasing stress, whereas in the results presented here, the yield point usually coincided with the maximum stress. Furthermore, Runza *et al.*[15] found a longer toe region for the bovine dura mater compared to the human dura mater. This indicates that there may be considerable variation in the

mechanical properties of dura mater between species and although bovine dura mater is frequently used in spinal biomechanical studies,[6,8,15,19] its use as a model for human tissue may be limited due to differences in mechanical properties. However, the findings of this study will assist in the development of more accurate models, in particular when bovine dura mater is employed.

In summary, no significant effect was found due to a 100-fold increase in strain rate on the mechanical properties of dura mater. Longitudinal specimens were found to be stronger and more deformable than circumferential specimens, although less stiff at low strains.

ACKNOWLEDGMENT

REFERENCES

[1]Atlas, S. W., V. Regenbogen, L. F. Rogers, and K. S. Kim. The radiographic characterization of burst fractures of the spine. *AJR Am. J. Roentgenol.* 147:575–582, 1986.

[2]Bilston, L. E., and L. E. Thibault. The mechanical properties of the human cervical spinal cord in vitro. *Ann. Biomed. Eng.* 24:67–74, 1996.

[3]Crisco, J. J., D. C. Moore, and R. D. McGovern. Strain-rate sensitivity of the rabbit MCL diminishes at traumatic loading rates. *J. Biomech.* 35:1379–1385, 2002.

[4]Elliott, D. M., D. A. Narmoneva, and L. A. Setton. Direct measurement of the Poisson's ratio of human patella cartilage in tension. *J. Biomech. Eng.* 124:223–228, 2002.

[5]Fiford, R. J., and L. E. Bilston. The mechanical properties of rat spinal cord in vitro. *J. Biomech.* 38:1509–1515, 2005.

[6]Hall, R. M., R. J. Oakland, R. K. Wilcox, and D. C. Barton. Spinal cord-fragment interactions following burst fracture: an in vitro model. *J. Neurosurg. Spine* 5:243–250, 2006.

[7]Hewitt, J., F. Guilak, R. Glisson, and T. P. Vail. Regional material properties of the human hip joint capsule ligaments. *J. Orthop. Res.* 19:359–364, 2001.

[8]Ichihara, K., T. Taguchi, I. Sakuramoto, S. Kawano, and S. Kawai. Mechanism of the spinal cord injury and the cervical spondylotic myelopathy: new approach based on the mechanical features of the spinal cord white and gray matter. *J. Neurosurg.* 99:278–285, 2003.

[9]Loth, F., M. A. Yardimci, and N. Alperin. Hydrodynamic modeling of cerebrospinal fluid motion within the spinal cavity. *J. Biomech. Eng.* 123:71–79, 2001.

[10]Maikos, J. T., R. A. Elias, and D. I. Shreiber. Mechanical properties of dura mater from the rat brain and spinal cord. *J. Neurotrauma* 25:38–51, 2008.

[11]Mazuchowski, E. L., and L. E. Thibault (2003). Biomechanical properties of the human spinal cord and pia mater. Summer Bioengineering Conference. Sonesta Beach Resort in Key Biscayne, FL, USA.

[12]Ogden, R. W. Large deformation isotropic elasticity—on the correlation of theory and experiment for incompressible rubberlike solids. *Proc. R. Soc. Lond. Ser. A Math. Phys. Sci.* 326:565–584, 1972.

[13]Patin, D. J., E. C. Eckstein, K. Harum, and V. S. Pallares. Anatomic and biomechanical properties of human lumbar dura mater. *Anesth. Analg.* 76:535–540, 1993.

[14]Reid, J. D. Effects of flexion-extension movements of the head and spine upon the spinal cord and nerve roots. *J. Neurol. Neurosurg. Psychiatry* 23:214–221, 1960.

[15]Runza, M., R. Pietrabissa, S. Mantero, A. Albani, V. Quaglini, and R. Contro. Lumbar dura mater biomechanics: experimental characterization and scanning electron microscopy observations. *Anesth. Analg.* 88:1317–1321, 1999.

[16]Tencer, A. F., B. L. Allen, Jr., and R. L. Ferguson. A biomechanical study of thoracolumbar spine fractures with bone in the canal. Part III. Mechanical properties of the dura and its tethering ligaments. *Spine* 10:741–747, 1985.

[17]Ting, T. C. T., and T. Chen. Poisson's ratio for anisotropic elastic materials can have no bounds. *Q. J. Mech. Appl. Math.* 58:73–82, 2005.

[18]Tunituri, A. R. Elasticity of the spinal cord dura in the dog. *J. Neurosurg.* 47:391–396, 1977.

[19]Wilcox, R. K., D. J. Allen, R. M. Hall, D. Limb, D. C. Barton, and R. A. Dickson. A dynamic investigation of the burst fracture process using a combined experimental and finite element approach. *Eur. Spine J.* 13:481–488, 2004.

[20]Wilcox, R. K., L. E. Bilston, D. C. Barton, and R. M. Hall. Mathematical model for the viscoelastic properties of dura mater. *J. Orthop. Sci.* 8:432–434, 2003.

[21]Woo, S. L., M. A. Gomez, and W. H. Akeson. The time and history-dependent viscoelastic properties of the canine medical collateral ligament. *J. Biomech. Eng.* 103:293–298, 1981.

[22]Yuan, Q., L. Dougherty, and S. S. Margulies. In vivo human cervical spinal cord deformation and displacement in flexion. *Spine* 23:1677–1683, 1998.